Influence of the behavioral goal and environmental obstacles on rapid feedback responses

Joseph Y. Nashed, Frédéric Crevecoeur and Stephen H. Scott

J Neurophysiol 108:999-1009, 2012. First published 23 May 2012;
doi: 10.1152/jn.01089.2011

J Neurophysiol 108: 999–1009, 2012.
First published May 23, 2012; doi:10.1152/jn.01089.2011.

Influence of the behavioral goal and environmental obstacles on rapid feedback responses

Joseph Y. Nashed,[1] Frédéric Crevecoeur,[1] and Stephen H. Scott[1,2,3]

[1]*Centre for Neuroscience Studies, Queen's University, Kingston, Ontario, Canada;* [2]*Department of Anatomy and Cell Biology, Queen's University, Kingston, Ontario, Canada; and* [3]*Department of Medicine, Queen's University, Kingston, Ontario, Canada*

Submitted 30 November 2011; accepted in final form 16 May 2012

Nashed JY, Crevecoeur F, Scott SH. Influence of the behavioral goal and environmental obstacles on rapid feedback responses. *J Neurophysiol* 108: 999–1009, 2012. First published May 23, 2012; doi:10.1152/jn.01089.2011.—The motor system must consider a variety of environmental factors when executing voluntary motor actions, such as the shape of the goal or the possible presence of intervening obstacles. It remains unknown whether rapid feedback responses to mechanical perturbations also consider these factors. Our first experiment quantified how feedback corrections were altered by target shape, which was either a circular dot or a bar. Unperturbed movements to each target were qualitatively similar on average but with greater dispersion of end point positions when reaching to the bar. On random trials, multijoint torque perturbations deviated the hand left or right. When reaching to a circular target, perturbations elicited corrective movements that were directed straight to the location of the target. In contrast, corrective movements when reaching to a bar were redirected to other locations along the bar axis. Our second experiment quantified whether the presence of obstacles could interfere with feedback corrections. We found that hand trajectories after the perturbations were altered to avoid obstacles in the environment. Importantly, changes in muscle activity reflecting the different target shapes (bar vs. dot) or the presence of obstacles were observed in as little as 70 ms. Such changes in motor responses were qualitatively consistent with simulations based on optimal feedback control. Taken together, these results highlight that long-latency motor responses consider spatial properties of the goal and environment.

reaching; spatial targets; optimal feedback control

REACHING MOVEMENTS to grasp and interact with objects in the environment must consider a variety of factors beyond the object's spatial location. For example, we can direct reaching movements to pick up a stick anywhere along its length, and we can easily reach around obstacles in our environment. It is well known that features such as end goal shape, size, and orientation can alter the kinematics of reaching (Lametti et al. 2007; Soechting 1984). Similarly, the presence of obstacles or distracters in the environment can alter hand trajectories during reaching (Chapman and Goodale 2008; Howard and Tipper 1997; Jackson et al. 1995; Lacquaniti et al. 1986). These results demonstrate the inherent sophistication of the voluntary motor system to plan and initiate motor actions. However, less is known on whether online feedback corrections share this sophistication.

Recent theories of voluntary motor control highlight the importance and potential sophistication of feedback processes during motor actions (Scott 2004; Todorov and Jordan 2002; Todorov 2004). Correspondingly, behavioral studies have begun to highlight considerable flexibility in the use of feedback to guide movement (Knill et al. 2011; Liu and Todorov 2007; Diedrichsen and Dowling 2009a; Diedrichsen and Gush 2009b; Franklin and Wolpert 2008; Prablanc and Martin 1992). With regard to properties of the spatial goal, Knill and colleagues (2011) demonstrated that motor responses to small shifts in visual feedback of hand motion during reaching varied for rectangular targets oriented in different spatial directions. Subjects corrected more for perturbations aligned with the narrow dimension of the target compared with perturbations aligned with the long dimension. Differences in hand motion based on target shape were observable between 150 and 200 ms. However, even faster online corrections may be possible as this study used visual shifts of hand position that did not engage much faster feedback processes related to muscle afferents. The fastest upper limb electromyographic (EMG) responses to visual stimuli occur at ~90 ms (Pruszynski et al. 2010), whereas limb afferent feedback can influence motor output in as little as 25 ms (Pierrot-Deseilligny and Burke 2005).

Muscle activity associated with feedback corrections to mechanical perturbations, previously termed rapid motor responses, can be generally divided into two components: short-latency responses (20–45 ms) and long-latency responses (45–105 ms) (for a review, see Pruszynski and Scott 2012). Short-latency responses are generated by the spinal cord and can be modified only under limited conditions (Wolpaw 1983; Wolf and Segal 1996; Christakos et al. 1983; Komiyama et al. 2000). In contrast, long-latency responses include a transcortical feedback pathway and have been shown to be modified by changes in task instruction (Rothwell et al. 1980; Pruszynski et al. 2008; Lewis et al. 2006; Lee and Tatton 1982; Hammond 1956; Crago et al. 1976), stability (Nichols and Houk 1976; Akazawa et al. 1983; Krutky et al. 2010), and joint dynamics (Lacquaniti and Soechting 1984; Lacquaniti and Soechting 1986; Kurtzer et al. 2008; Kurtzer et al. 2009). Thus, these studies highlight the ability of corrective responses to consider the nominal goal and features of the motor periphery. We hypothesize that, as observed in voluntary control, these corrective responses will also consider more complex issues related to the properties of the goal and environment as voluntary control and transcortical feedback pathways involve similar neural substrates (Scott 2004, 2008).

In this report, we explore whether rapid motor responses are altered to account for spatial constraints associated with the size of the end goal and the presence of obstacles in the

Address for reprint requests and other correspondence: J. Y. Nashed, Centre for Neuroscience Studies, Botterell Hall, Rm. 232, Queen's Univ., Kingston, Ontario, Canada K7L 3N6 (e-mail: 0jn9@queensu.ca).

environment, similar to voluntary motor control. We developed an optimal control model to characterize how these factors may influence motor patterns and found that subjects generated qualitatively similar corrective responses. Critically, task-specific changes in motor responses consistent with the simulations were observed in as little as 70 ms, showing that high-level factors of movement planning, such as target shape and the presence of obstacles, modulate feedback responses to perturbations within the long-latency epoch.

METHODS

Participants

A total of 35 subjects (20 men and 15 women, age: 21–35 yr, 19 right hand dominant) participated in 3 experiments. Six subjects participated in *experiments 1* and *3*, whereas one subject participated in *experiments 1* and *2*. Sixteen of the thirty-five subjects were recruited to participate in the randomization variants of *experiments 1* and *2*. All subjects were neurologically healthy and gave informed consent according to a protocol approved by the Research Ethics Board of Queen's University. Experiments did not exceed 2 h, and subjects were compensated for their time.

Apparatus and Experimental Design

As described in our previous studies (Kurtzer et al. 2008; Pruszynski et al. 2008; Scott 1999), experiments used a robotic device (KINARM Exoskeleton, BKIN Technologies, Kingston, ON, Canada) permitting elbow and shoulder movement in the horizontal plane. In addition to recording flexion/extension movement of each joint, the KINARM can displace the arm by applying mechanical loads. Projected target lights and hand feedback (white dot, 0.5-cm diameter) were presented to the subject from a heads-up display consisting of an overhead projector and a semitransparent mirror. During the experiment, direct vision of the arm and hand was occluded by a metal partition.

Muscle Recordings

Surface EMG recordings were obtained from the following flexor and extensor muscles of the elbow and shoulder: brachioradialis (Br; elbow flexor), triceps lateral (TLat; elbow extensor), deltoid posterior (DP; shoulder extensor), and pectoralis major (PM; shoulder flexor). Full details of the procedures are described in our earlier studies (Kurtzer et al. 2008; Pruszynski et al. 2008).

Experiments

Experiment 1: influence of target shape on feedback corrections during reaching. This experiment examined the flexibility of feedback corrections after mechanical perturbations during reaching to a small circular target or an elongated horizontal bar. Subjects (n = 10) initiated their hand movements from a small start target (radius: 0.5 cm), such that the shoulder and elbow angles were ~20 and 110°, respectively. Subjects were required to perform 20-cm reaching movements directly ahead (Fig. 1*A*) to one of two end targets: *1*) a circular dot (radius: 0.5cm) or *2*) a rectangular bar (length: 80 cm). Upon trial completion, subjects were notified as to whether they attained predetermined speed and accuracy criteria [successful: end target filled green; failures: too fast (<700 ms, end target filled red), or too slow (>1,000 ms, end target filled yellow)]. On random trials, step torques were applied to the limb when the hand was 5 cm beyond the start target. Either flexion/flexion (elbow: 2 N·m, shoulder: 2 N·m) or extension/extension (elbow: 0.5 N·m, shoulder: 2 N·m) torques were applied, which deviated the hand to the left and right, respectively. The above joint torques were chosen to produce qualitatively similar hand path deviations to the left and right. Subjects readily compensated for these loads to attain the spatial targets (see RESULTS). Subjects performed each condition (dot or bar) in a blocked fashion. Blocks included 5 repeats of each perturbation randomized with 40 nonperturbation trials, for a total of 50 trials/block. The target conditions were presented three times interleaved, with the first block randomly selected from one of the target conditions (15 perturbation trials in total for each target condition). Subjects were given a few practice trials before data collection to become generally familiar with the task and the loads (~5 perturbed trials).

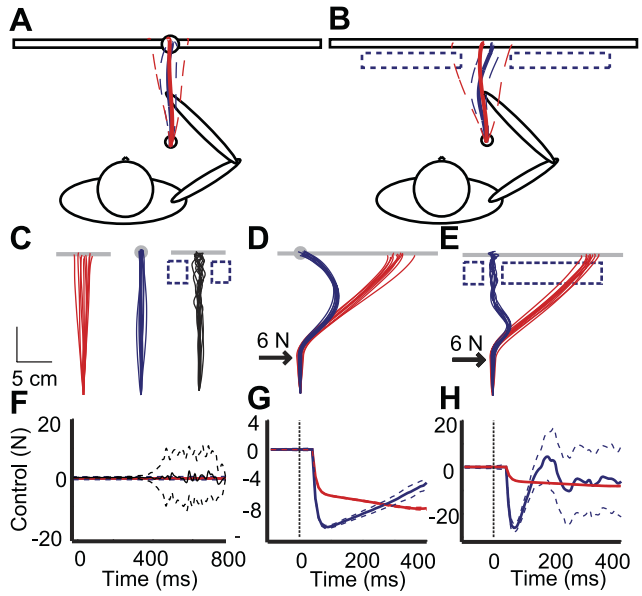

Fig. 1. Schematic description of the experimental protocol and predictions. *A*: empirical data from *experiment 1*. Shown are means (solid line) and SDs (dashed lines) of all subjects illustrating the reaching movements made to one of two end targets, either a circular dot (blue; radius: 0.05 cm) or a rectangular bar (red; length: 80 cm and width: 3 cm), located directly 20 cm in front of the start target (radius: 0.5 cm). *B*: empirical data from *experiment 2*. Shown are means (solid lines) and SDs (dashed lines) of all subjects illustrating the reaching movements made to the rectangular bar with (blue) and without (red) obstacles in the environment. *C–H*: simulated results. *C*: Predicted unperturbed movement trajectories for the dot (red), bar (blue), and obstacle (black) conditions based on the optimal control policy. *D*: predicted feedback correction after a rightward perturbation for each target type based on the optimal control policy. *E*: predicted feedback correction after a rightward perturbation with and without obstacles based on the optimal control policy. *F*: predicted control policies for the bar (red), dot (blue), and obstacle (black) conditions based on the optimal control policy. Note that the control signals for the bar and dot were much smaller compared with the obstacle condition. *G*: predicted control policies after a rightward perturbation for each target type based on the optimal control policy. *H*: predicted control policies after a rightward perturbation with and without the presence of obstacles based on the optimal control policy.

For each muscle, perturbation direction, and target condition, we quantified learning in the long-latency epoch over the course of the perturbed trials. This was achieved by taking the mean long-latency response of the early (mean of the first three) and late (mean of the last three) perturbed trials for each subject and performing a paired t-test between these two values.

To rule out any stimulus-specific learning in the previous blocked paradigm, a random trial-by-trial variation of the task was performed. Thus, in addition to the experiment described above, additional subjects (n = 8) performed the same task in a randomized fashion as opposed to the blocked structure described above. In other words, subjects were presented with either the bar or dot randomly on each trial. Similar to above, they performed 15 repeats of each perturbation condition.

Experiment 2: influence of obstacles on feedback corrections during reaching. This experiment examined the flexibility of feedback corrections during reaching with and without obstacles in the environment. The experimental protocol was similar to the bar condition of *experiment 1*; however, subjects ($n = 10$) performed reaches with and without the added constraints of obstacles placed within the workspace. Two parallel obstacles, separated by 10 cm, were strategically located to the right and left of the unperturbed hand trajectory of *experiment 1* (Fig. 1*B*). Importantly, the obstacles were positioned so they did not obstruct the unperturbed reaching trajectories of *experiment 1*. Collision with an obstacle resulted in haptic feedback such that a repulsive force was generated, which impeded hand movement. On perturbation trials, uncorrected movements resulted in hand paths being impeded by one of the two obstacles. Subjects performed each condition (obstacles or no obstacles) in a blocked fashion, such that each block included 5 repeats of the perturbation conditions randomized with 40 nonperturbation trials, for a total of 50 trials/block. Obstacle and no obstacle conditions were presented three times interleaved, with the first block randomly selected (15 perturbations trials in total for each condition). Subjects were given a few practice trials before data collection to become generally familiar with the task, the loads, and the properties of the virtual obstacles (~5 perturbed trials). A second variant of this task was also performed in which the subjects reached to the circular dot rather than the bar. We also quantified learning in the long-latency epoch in a similar fashion to *experiment 1*. In addition, eight subjects performed this task where trials with or without obstacles were randomly interleaved.

Experiment 3: influence of tonic muscle activity on feedback corrections. We noted some changes in background muscle activity between obstacle conditions (see RESULTS). Thus, the purpose of this experiment was to examine the effects of changes in tonic muscle activity upon rapid motor corrections during reaching. Directly controlling for changes in cocontraction is difficult; thus, we artificially induced increases in muscular activity by selectively applying background loads. The experimental protocol was similar to the circular dot condition of *experiment 1*. Subjects ($n = 6$) maintained their hand in the start target against one of three possible background loads (−2, 0, and 2 N·m) applied to both the shoulder and elbow, exciting either the flexors or extensors. Perturbations were applied similar to *experiment 1*. Subjects performed 15 repeats of each perturbation condition (2 directions) for each background load (3 background loads) for a total of 90 perturbed trials. As all combinations of loads and perturbation types were examined, subjects could not anticipate perturbation direction. Perturbation trials were randomized with 210 nonperturbed trials, for a total of 300 trials.

Model

We considered the translation of a unit point mass ($m = 1$) in the horizontal plane in the presence of three forces: a viscous force proportional to the two-dimensional velocity with opposite sign, a controlled force (F), and an external force (F_{ext}). To approximate the muscle dynamics, we assumed a first-order linear filter between the control variable and the controlled force coupled with the differential equation describing the translation of the point mass. The external force was assumed to be constant. The control system was therefore given by the following differential equation:

$$m\ddot{p} = -G\dot{p} + F + F_{ext} \quad (1)$$

$$\tau\dot{F} = u - F \quad (2)$$

$$\dot{F}_{ext} = 0 \quad (3)$$

where m is mass, $p(t)$ is the two-dimensional coordinate vector of the point mass in the plane, G is the viscous constant, F and F_{ext} are the two-dimensional controlled and external forces, respectively, and u is the two-dimensional control vector. G was set to 1 $N \cdot s \cdot m^{-1}$, and the time constant of the linear filter (τ) was set to 40 ms, which is compatible with the first approximation of muscle dynamics (Brown and Loeb 2000). m and G were arbitrarily set to unit values to standardize the simulations. These parameters have qualitatively no influence on the simulation results. To introduce stochastic dynamics and noise disturbances, the continuous time system was transformed into a discrete time system of the following form using classical transformation methods of linear ordinary differential equations and an explicit Euler integration scheme with a 10-ms time step:

$$x_{k+1} = Ax_k + Bu_k + \text{motor noise} \quad (4)$$

where x_{k+1} is the state vector at time $k + 1$, A and B are matrices that describe the system dynamics, and u_k is the control signal at time k. The state vector containing the position, velocity, and forces was augmented with a vector of the same dimension that contained the target state (16 dimensions). Finally, we further augmented the state vector with the previous states to take feedback delays into account and reduce the delayed feedback signal to the nondelayed case by letting the controller observe only the most delayed state. This technique is a classical procedure used to handle discrete systems subject to fixed delays (Mehta and Schaal 2002; Todorov and Jordan 2002; Izawa and Shadmehr 2008; Crevecoeur et al. 2010).

Under these assumptions, the feedback signal at each time step (y_k) can be written as follows:

$$y_k = x_{k-h} + \text{sensory noise} \quad (5)$$

or, equivalently,

$$y_k = H\left(x_k^T, x_{k-1}^T, \ \ldots\ , x_{k-h}^T\right)^T + \text{sensory noise} \quad (6)$$

where h is the feedback delay expressed in number of time steps, the observability matrix (H) = $(0\ 0 \ldots I_{16\times16})$, and T is the transpose. This delay was set to 50 ms (5 time steps) to reflect the transmission delay associated with the long-latency response. After reducing the system to the nondelayed case, we can use an optimal linear state estimator (Kalman filter) that consists in weighting prior beliefs about the state of the system with sensory feedback to derive a maximum likelihood estimate of the system state. In practice, let $\hat{x}_k$ be the estimated state at time k (including the target and past states). Thus, the prior belief about the next state is as follows:

$$\hat{x}_{k+1}^P = A\hat{x}_k + Bu_k + \text{prediction noise} \quad (7)$$

and the feedback correction yields the full state estimate by taking y_{k+1} into account:

$$\hat{x}_{k+1} = \hat{x}_{k+1}^P + K_{k+1}(y_{k+1} - H\hat{x}_{k+1}^P) \quad (8)$$

The sequence of Kalman gains (K_i) must be computed.

The motor noise affected the force production only and was composed of two terms: an additive term plus a control-dependent term with principal axis aligned with the direction of the control vector with variance $(0.015)^2 \times u$ and a secondary axis orthogonal to the control vector with variance $(0.005)^2 \times u$ (Liu and Todorov 2007). The sensory noise was additive and affected all components of the most delayed state, including the target. The prediction noise was also additive. It affected only the estimate of the next time step and, therefore, not the history of the process stored in the augmented state vector. The covariance matrixes of additive, predictive, and feedback noises were all diagonal matrixes. The variance of the additive motor noise was set to 10^{-2}, and the variances of the feedback and prediction noises (when they are nonzero for the prediction disturbance) were set to 10^{-6}.

The optimal control variables and optimal Kalman gains depend on the task that was expressed by the cost function that the controller must minimize along the trajectory. A control-dependent cost was applied to all simulation runs such that at each time step, the cost of control was equal to $10^{-6} \times \|u_k\|^2$. To simulate the unperturbed

reaching to a circular target, we used a terminal cost function such that:

$$\text{final cost} = \|p - p^*\|^2 + \|\dot{p} - \dot{p}^*\|^2 \quad (9)$$

where the two dimensions of the plane were constrained. The same cost function was used to simulate the reaching toward a bar except that only one dimension of the plane was penalized and there was no cost associated with deviations along the axis of the bar target (we note p_x the coordinate along this axis). The two-dimensional velocity penalty was unchanged across the simulated reaches toward the bar or circular target to express that the movement had to stop at the end of the simulation run. To simulate the perturbations, the lateral component of the external force was changed within each simulation run when the distance travelled by the point mass exceeded 5 cm, using the same position threshold as in the experimental paradigm. Finally, the obstacles were approximated as an extremely high penalty on the deviations orthogonal to the reach path during the last portion of the movement, when subjects approached the edges of the obstacles. This penalty was expressed as follows: $100(p_x - p_x^*)^2$. Based on subjects' data, the controller had to drive the point mass to the goal in 800 ms and the presence of constraints simulating the obstacles occurred after 500 ms.

With these definitions of system dynamics, feedback signals, noise parameters, and cost functions, we computed the optimal feedback gains and adaptive Kalman gains associated with each target and obstacle condition following algorithms adapted to the presence of control-dependent noise (Todorov 2005; Crevecoeur et al. 2011).

Since the plant dynamics are linear and the cost function is quadratic, the optimal feedback control policy turned out to be a linear function of the following estimated state:

$$u_k = -L_k \hat{x}_k \quad (10)$$

where L_k represents the optimal feedback gains. These hypotheses are a simplification of the motor system, but the resulting control algorithm presents the advantage of expressing the control variable as an explicit function of the estimated state. In more general settings (including nonlinear dynamics and arbitrary cost functions), the optimal control policy is also a function of the system state, but it is practically impossible to compute due to the computational complexity that grows exponentially as the system dimension increases. To the best of our knowledge, current numerical techniques are based on iterative improvements of locally optimal control policies computed in the neighborhood of a nominal trajectory (Li and Todorov, 2007).

Each model was used for trials with and without perturbations. The different cost and noise parameters were standard values chosen to produce simulation results that were in general agreement with the experimental results. We verified that these parameters did not qualitatively influence the dependency of the feedback response on task requirements.

Data Analysis

Filtering and normalization. All data were aligned on the perturbation onset. Kinematic and EMG data were processed in the following manner: joint angles and hand positions were low-pass filtered (20 Hz, two pass, sixth-order Butterworth). All EMG signals were band-pass filtered (25–250 Hz, two pass, sixth-order Butterworth) and full wave rectified. EMG was normalized by its mean activity in a separate set of trials where subjects maintained a constant posture against 1-N·m torques applied to each joint individually.

Behavior and kinematics. Receiver operator curves (ROCs) were used to determine significant differences in corrections based on tangential velocity (Green and Swets 1966). ROC areas were computed on the distribution of individual trials for each subject, and the resulting time series were averaged across them. The ROC curve represents the probability at each time point (1 ms) that an ideal observer could discriminate between categories or conditions. Values of 0 and 1 indicate perfect discrimination; in contrast, a value of 0.5 is indicative of performance at chance. Significant discrimination was determined when the first ROC area remained <0.25 or >0.75 for five consecutive time samples (Corneil et al. 2004; Pruszynski et al. 2008).

We used subject means and performed paired *t*-tests to determine significant differences in the terminal hand and joint positions. Terminal positions were defined as the final position of the hand within the end target. We compared subject means of the hand (*x*-direction), elbow, and shoulder joint position for similar perturbations between different target (bar vs. dot) and obstacle (with vs. without) conditions. Similarly, we examined the lateral variability (SD, *x*-direction) of each subject's terminal hand position for the unperturbed reaching movements and compared them between target and obstacle conditions to quantify differences in end point distributions.

Muscle activity. Our primary interest was to compare different epochs of muscle activity to gain further insight into the sensitivity of feedback responses to spatial goals and environmental constraints (obstacles). The epochs of muscle activity of most interest were based on previous reports (Crago et al. 1976; Lee and Tatton 1975; Mortimer et al. 1981; Nakazawa et al. 1997) and were categorized temporally: baseline = −100 to 0 ms, R1 = 20–45 ms, R2 = 45–75 ms, R3 = 75–105 ms, and voluntary (Vol) = 120–180 ms. The R1-R3 convention is similar to the M1-M3 convention proposed by Lee and Tatton (1975) but should avoid confusion with the earliest response (R1; previously M1) and primary motor cortex's common abbreviation (M1).

Our experimental design allowed us to make straightforward comparisons between conditions to determine if feedback responses modulate as a function of task demands. Paired *t*-tests were performed using subject means to determine changes for similar perturbations between the different target (dot vs. bar) and obstacle (with vs. without) conditions. We were most interested in comparing the perturbation-related muscle activity between experimental conditions of each subject. Accordingly, we calculated subject means for each experimental condition and subsequently used the change in activity between the perturbed and unperturbed conditions, which is ultimately what we consider the perturbation-related muscle activity.

RESULTS

Experiment 1: Influence of Target Shape on Feedback Corrections During Reaching

The optimal control model predicted that the pattern of hand trajectories would be different whether the target was circular or a long horizontal. Specifically, the end point distribution when reaching to a bar is much broader than when reaching to a circular target (Fig. 1*C*). This difference in end point distributions is a consequence of the task-specific cost function that leaves the dimension orthogonal to the reach path not penalized when reaching to a bar. The greater variability in the control variable associated with reaching to a circular target shows that the deviations along the orthogonal axis are taken into account and corrected by the controller.

Qualitatively similar results were observed for human subjects for these unperturbed reaching trials. Unperturbed reaches to the circular dot were relatively straight with bell-shaped velocity profiles (Fig. 1*A*). Although subjects could reach anywhere along the horizontal bar, they chose reaching movements straight ahead to the goal (Fig. 1*A*). Accordingly, initial hand paths overlapped greatly between the two conditions (bar and dot). A notable difference was the larger terminal variability associated with the bar (end point SD = 2.5 cm) compared with the dot (end point SD = 0.4cm, $t_9 = 4.88$, $P = 0.008$).

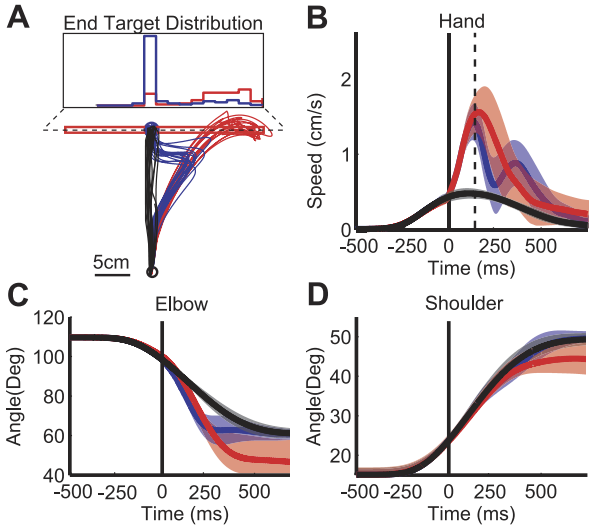

Fig. 2. Limb kinematics during reaching in *experiment 1* with extensor torque perturbations. *A*: hand motion from an exemplar subject during reaching to the circular dot (blue) or rectangular bar (red). The black lines represent the unperturbed trajectories to the circular dot. The horizontal dotted line indicates the 20-cm point at which the above distributions were obtained. Note that the unperturbed trajectories to the bar have been omitted for clarity. *Top*: positional cross-section. The lateral distributions indicate the first crossing of the 20-cm position of all trials from all subjects. *B*: mean (solid lines) and SD (shaded regions) speed profiles over time for the same reaching movements. The dashed line indicates the first point of statistical difference in the velocity profiles determined by receiver operator curve (ROC) analysis. *C*: mean (solid lines) and SD (shaded regions) of elbow angles versus time for the same reaching movements. *D*: mean (solid lines) and SD (shaded regions) of shoulder angles versus time for the same reaching movements. Data were aligned to the perturbation onset with the vertical line indicating the perturbation onset. Red and blue lines correspond to the circular dot and rectangular bar, respectively.

Figure 1*D* highlights the response generated by the optimal control model to this perturbation. The simulations reveal that even if the mass is free to move until the final time step, the controller directly responds to the change in external force (Fig. 1*D*). Importantly, the target shapes yield very different initial responses, with a larger response required for the circular target and a smaller response for the horizontal bar (Fig. 1*G*). A reduced response associated with the bar is predicted as the goal can be attained with less effort by redirecting object motion to the right side of the bar. This nontrivial result reflects that although there is not a penalized path, delaying the response would result in an expensive need for higher motor commands that is suboptimal (Fig. 1, *F* and *H*). The best strategy is to compensate for changes in external forces while taking target shape into account as early as possible.

In human subjects, the limb was unexpectedly perturbed by either flexor or extensor torques in 20% of trials, which displaced the hand to the left or right, respectively. The amount of forward acceleration varied for both torque conditions due to intersegmental dynamics. The extensor torques predominantly caused an increase elbow extension deviating the hand rightward, away from the circular dot, and rapid corrections were made directly toward the target (Fig. 2*A*). In contrast, there was little corrective movement of the hand trajectories for these extensor torques when subjects reached to the horizontal bar. ROC analysis revealed differences in tangential velocities for the two types of targets at 184 ms (Fig. 2*B*). Significantly different terminal hand (Fig. 2*A*) and joint (Fig. 2, *C* and *D*) positions were observed between target conditions ($P < 0.001$).

The perturbation-related muscle activity was quantified for each subject by taking the difference between the mean of the perturbed trials and the mean of the unperturbed trials (Kurtzer et al. 2009). Figure 3 shows the changes in muscle activity in the Br and PM muscles for the dot and bar after extensor torques for an exemplar subject (Fig. 3*A*) and for the group (Fig. 3*B*). The R2, R3, and Vol epochs were all elevated from baseline and exhibited greater modulation for the dot compared with the bar for both PM (R2: $t_9 = 2.29$, $P = 0.045$; R3: $t_9 = 2.84$, $P = 0.018$; Vol: $t_9 = 3.45$, $P = 0.006$) and Br (R2: $t_9 = 3.29$, $P = 0.008$; R3: $t_9 = 3.99$, $P = 0.003$; Vol: $t_9 = 3.04$, $P = 0.013$; Fig. 3*C*). Thus, the large corrective movement of the hand back to the circular target was generated by increases in PM and Br activity that began during the long latency time epoch. Notably, the R1 epoch was the only binned epoch not significantly elevated from baseline and did not exhibit differences between the dot and bar in either muscle (PM: $t_9 = 1.70$, $P = 0.120$; Br: $t_9 = 0.90$, $P = 0.340$; Fig. 3*C*). Importantly, we found no learning effects across trials for rightward perturbations in either the bar or dot conditions in any of the active muscles (those that generated corrective movements, $P > 0.05$ by paired *t*-test, for all muscles).

We found essentially the same results when flexor torques displaced the hand leftward during reaching (Fig. 4). However, unlike the extension torques, flexor torques caused deviations from the initial trajectories at both the shoulder and elbow joints. Subjects made a single corrective movement directly toward the circular dot. In contrast, hand trajectories to the rectangular bar resulted in smaller corrections as movements were redirected toward another location on the bar. Differences in tangential velocities for the two target types were observed at 196 ms using ROC analysis. Furthermore, significantly

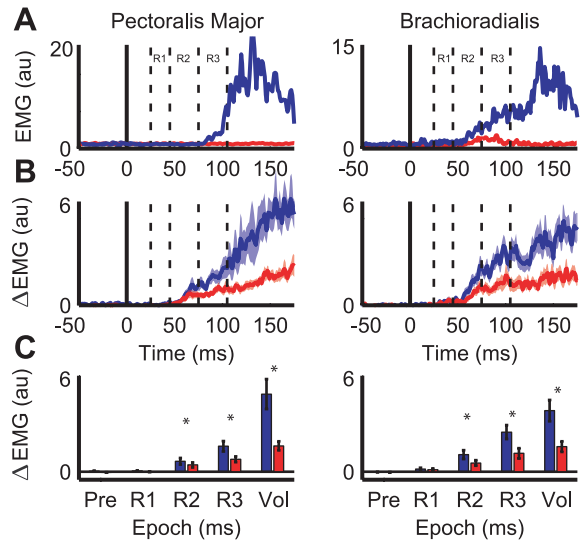

Fig. 3. Flexor muscle activity of the brachioradialis (*right*) and pectoralis major (*left*) muscles after extension torque perturbations. *A*: mean muscle activity from an exemplar subject aligned to the perturbation onset. The blue and red traces indicate the mean muscle activity in the circular dot and rectangular bar, respectively. The solid vertical line marks the perturbation onset. EMG, electromyograph; au, arbitrary units. *B*: mean (solid lines) and SE (shaded regions) perturbation-evoked muscle activity of the group, obtained by subtracting each subject's unperturbed muscle activity from their perturbed muscle activity and then averaging across subjects. *C*: bar plots of evoked muscle activity within the different epochs. The vertical height and error bars indicate the group means and SEs. Pre, baseline; Vol, voluntary. *$P < 0.05$.

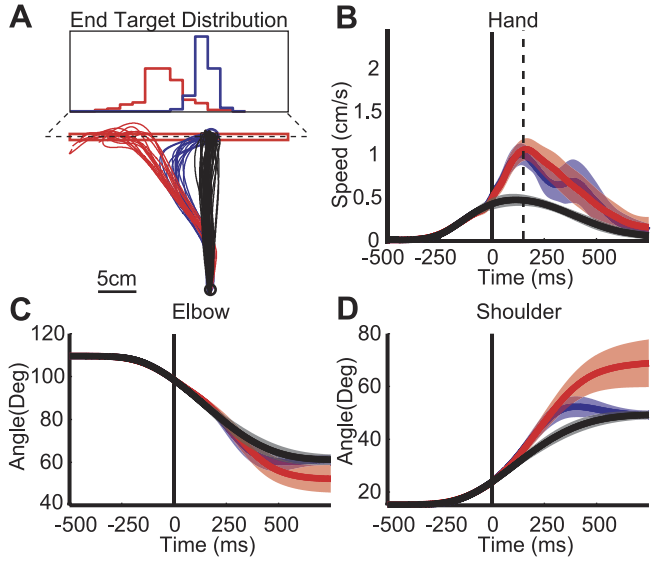

Fig. 4. Limb kinematics during reaching in *experiment 1* with flexor torque perturbations. *A*: hand motion from an exemplar subject during reaching to the circular dot (blue) and rectangular bar (red). The black line represents the unperturbed trajectories to the circular dot. Note that unperturbed trajectories to the bar were omitted for clarity. *Top*: positional cross-section. The lateral distributions indicate the first crossing of the 20-cm position of all trials from all subjects. *B*: mean (solid lines) and SD (shaded regions) speed profiles over time for the same reaching movements. The dashed line indicates the first point of statistical difference in the velocity profiles determined by ROC analysis. *C*: mean (solid lines) and SD (shaded regions) of elbow angles versus time for the same reaching movements. *D*: mean (solid lines) and SD (shaded regions) of shoulder angles versus time for the same reaching movements. Data were aligned to the perturbation onset with the vertical line indicating the perturbation onset. Red and blue lines correspond to the circular dot and rectangular bar, respectively.

different terminal hand positions were observed for each target condition ($t_9 = 9.48$, $P < 0.001$).

Perturbation-related EMG activity for the DP and Tlat muscles was clearly observed for these imposed flexor torques (Fig. 5). The R2, R3, and Vol epochs were elevated from baseline and exhibited greater activity for the circular dot compared with the rectangular bar for both Tlat (R2: $t_9 = 2.83$, $P = 0.018$; R3: $t_9 = 2.29$, $P = 0.045$; Vol: $t_9 = 2.30$, $P = 0.044$) and DP (R2: $t_9 = 2.21$, $P = 0.047$; R3: $t_9 = 2.29$, $P = 0.045$; Vol: $t_9 = 3.03$, $P = 0.013$). Again, the R1 epoch of time was not significantly elevated from baseline, nor did it exhibit any target-related differences in either muscle (Tlat: $t_9 = -0.290$, $P = 0.778$; DP: $t_9 = 1.14$, $P = 0.282$). Similar to the rightward perturbation, we observed no learning effects in the long-latency epoch over the course of trials for leftward perturbations in either target condition ($P > 0.05$ by paired *t*-test, for all muscles).

Randomly interleaved trials with different target shapes. The results described above focused on data collected in a blocked fashion (i.e., blocks of reaching trials to a circular dot separated from trials to a bar). Here, we examine data collected in which target presentation was randomized. The observed behavior was essentially the same in this randomized condition. Terminal variability in unperturbed trials was greater for reaches to the bar (end point SD = 1.6 cm) compared with the circular dot (end point SD = 0.4 cm, $t_7 = 4.3$, $P = 0.008$). ROC analyses demonstrated differences in tangential hand velocity between bar and dot trials at 190 ms for rightward perturbations and 198 ms for leftward perturbations.

Similar to the blocked design, the upper limb muscle exhibited an increasing sensitivity to target type during the randomized trials (bar vs. dot). Again, the R1 response exhibited no difference between target conditions ($P > 0.05$ by paired *t*-test). In contrast, the R2, R3, and Vol epochs were significantly different between target conditions for all muscles ($P < 0.05$ by paired *t*-test). Thus, subjects could modify their corrective response from trial to trial based on the presented properties of the goal. We also compared the group EMG (R1, R2, R3, and Vol) results of the randomized and blocked designs and found no significant differences between the two groups ($F_{1,17} = 2.04$, $P = 0.371$, by MANOVA).

Experiment 2: Influence of Obstacles on Feedback Corrections During Reaching

Subjects reached to a horizontal bar with and without obstacles in the workspace to examine the flexibility of feedback responses with respect to environmental/trajectory constraints. As in experiment 1, unperturbed reaches without obstacles were relatively straight with bell-shaped velocity profiles (Fig. 1*B*). Similar hand paths were observed when obstacles were present in the environment, although the variability of hand paths was less with obstacles (end point SD = 1.06 cm) than without obstacles (end point SD = 3.90 cm, $t_9 = 5.72$, $P < 0.013$). A similar difference in end point positions was observed for movements with and without obstacles for the optimal control model (Fig. 1*C*).

Like target shape, the presence of obstacles altered how the optimal control model responded to mechanical perturbations. Reaching in the presence of obstacles creates additional constraints on the lateral deviations that produce vigorous corrections for the perturbation and more variable control signals

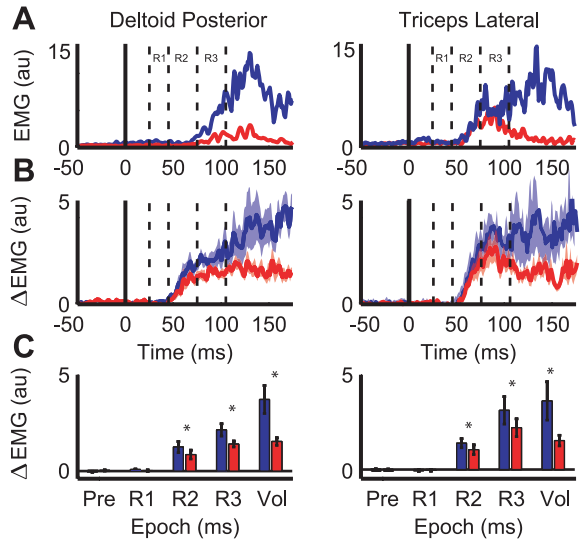

Fig. 5. Extensor muscle activity of the triceps lateral (*right*) and posterior deltoid (*left*) muscles after flexor torque perturbations. *A*: mean muscle activity from an exemplar subject aligned to the perturbation onset. The blue and red traces indicate the mean muscle activity in the circular dot and rectangular bar, respectively. The solid vertical line marks the perturbation onset. *B*: mean (solid lines) and SE (shaded regions) perturbation-evoked muscle activity of the group, obtained by subtracting each subject's unperturbed muscle activity from their perturbed muscle activity and then averaging across subjects. *C*: bar plots of evoked muscle activity within the different epochs. The vertical height and error bars indicate the group means and SE. *$P < 0.05$.

while moving between the obstacles, as the controller must correct any deviation toward them (Fig. 1, *E* and *H*).

When muscle activity on all trials with obstacles (PM = 0.58 ± 0.19, Br = 0.36 ± 0.16, Tlat = 0.49 ± 0.11, and DP = 0.35 ± 0.20; normalized means ± SD across all subjects) was compared with all trials without obstacles (PM = 0.47 ± 0.16, Br = 0.29 ± 0.14, Tlat = 0.39 ± 0.14, and DP = 0.29 ± 0.11; normalized means ± SD for across subjects), we observed a small (~15–20%) but significant increase in baseline muscle activity ($P < 0.05$ by paired *t*-test, for all muscles) before movement onset. Our analysis focused on analyzing the stretch response of the muscle relative to the baseline. By subtracting the mean of the unperturbed reaching trajectories from that of the mean of the perturbed trials, we effectively removed any increases in tonic muscle activity and isolated the evoked responses. A careful examination of the effect of changes in tonic muscle activation was performed in *experiment 3*.

On random trials, the limb was unexpectedly perturbed with extensor torques that deviated the hand rightward from its intended trajectory. Corrective movements without obstacles were similar to those produced in *experiment 1*. In contrast, when obstacles were present, subjects vigorously corrected back toward the central opening between the two obstacles (Fig. 6, *A* and *C*). ROC analysis revealed differences in tangential velocities at 135 ms between conditions (Fig. 6*B*). Significantly different terminal hand positions were observed between conditions ($t_9 = 9.80$, $P < 0.001$).

Extensor torques produced a rapid EMG response in the Br and PM muscles, as shown for an exemplar subject (Fig. 7*A*) and the group (Fig. 7*B*). Larger perturbation responses were observed

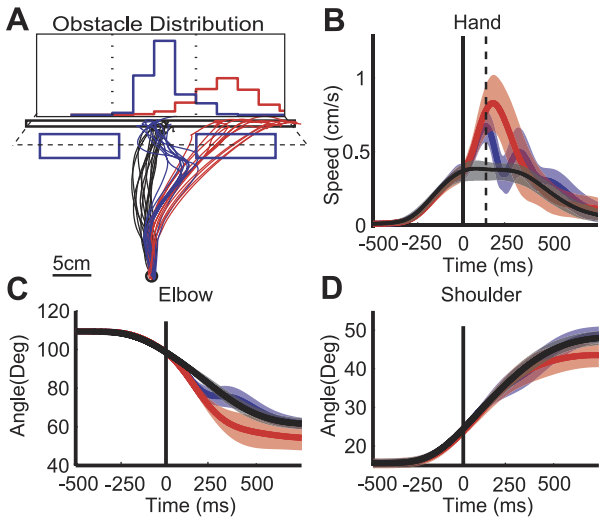

Fig. 6. Limb kinematics during reaching in *experiment 2* with extensor torque perturbations. *A*: hand motion from an exemplar subject during reaching with obstacles (blue) and without obstacles (red). The black lines illustrate the unperturbed trajectory to the bar. The horizontal dotted line indicates the obstacle midpoint (16.5cm) at which the above distributions were obtained. *Top*: positional cross-section. The lateral distributions indicating the first crossing of the obstacle midpoint position of all trials from all subjects. *B*: mean (solid lines) and SD (shaded rgions) speed profiles over time for the same reaching movements. The dashed line indicates the first point of statistical difference in the velocity profiles determined by ROC analysis. *C*: mean (solid lines) and SD (shaded regions) of elbow angles versus time for the same reaching movements. *D*: mean (solid lines) and SD (shaded regions) of shoulder angles versus time for the same reaching movements. Data were aligned to the perturbation onset with the vertical line indicating the perturbation onset. Red and blue lines correspond to the circular dot and rectangular bar, respectively.

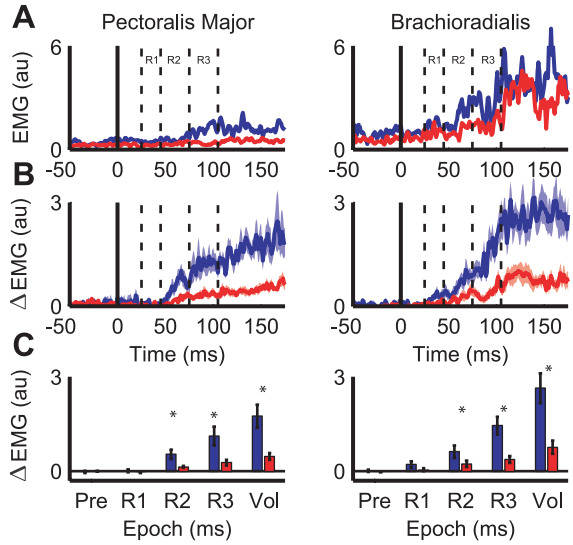

Fig. 7. Flexor muscle activity of the brachioradialis (*right*) and pectoralis major (*left*) muscles after extension torque perturbations. *A*: mean muscle activity from an exemplar subject aligned to the perturbation onset. The blue and red traces indicate the mean muscle activity in the circular dot and rectangular bar, respectively. The vertical line marks the perturbation onset. *B*: mean (solid lines) and SE (shaded regions) perturbation-evoked muscle activity of the group obtained by subtracting each subject's unperturbed muscle activity from their perturbed muscle activity and then averaging across subjects. *C*: bar plots of evoked muscle activity within the different epochs. The vertical height and error bars indicate the group means and SEs. *$P < 0.05$.

when the subjects reached with obstacles present compared with when obstacles were absent in the environment (Fig. 7*C*). More specifically, the R2, R3, and Vol epochs were all elevated and exhibited greater modulation for the obstacles compared with without for both PM (R2: $t_9 = 2.516$, $P = 0.033$; R3: $t_9 = 3.36$, $P = 0.008$; Vol: $t_9 = 3.07$, $P = 0.013$) and Br (R2: $t_9 = 2.73$, $P = 0.023$; R3: $t_9 = 5.29$, $P = 0.001$; Vol: $t_9 = 4.24$, $P = 0.002$; Fig. 6*D*). As in *experiment 1*, the R1 epochs of the perturbation-related activity for either flexor muscle was not significantly elevated whether obstacles were present or not (PM: $t_9 = 1.24$, $P = 0.247$; Br: $t_9 = 1.92$, $P = 0.087$). Similar to *experiment 1*, we found no learning effects across trials for rightward perturbations with or without the presence of obstacles ($P >> 0.05$ by paired *t*-test, for all muscles).

Comparable results were observed when flexor torques displaced the hand leftward. Without the presence of obstacles in the environment, subject's hand trajectories did not return to the center of the bar where unperturbed reaches were made. Rather, the hand was redirected to the left side of the bar, in the direction of the perturbation ($t_9 = 7.28$, $P < 0.001$). Conversely, when obstacles were present in the environment, subjects made a single corrective movement to navigate between the obstacles to reach the end goal. Differences in hand trajectories with obstacles versus without obstacles were observed at 142 ms using ROC analysis.

Increases in EMG for the DP and Tlat muscles were observed for the imposed flexor torques. Perturbation-related activity in the R2, R3, and Vol epochs of DP were greater in the presence of obstacles compared with without (R2: $t_9 = 4.13$, $P = 0.003$; R3: $t_9 = 3.22$, $P = 0.010$; Vol: $t_9 = 5.11$, $P = 0.001$). Tlat showed only a significant increase in activity for R2 and no significant increases in activity for the R3 and Vol epochs (R2: $t_9 = 2.35$, $P = 0.043$; R3: $t_9 = 1.87$, $P = 0.094$;

Vol: $t_9 = 2.21$, $P = 0.055$). Again, the R1 epoch of time was not significantly elevated from the corrected baseline, nor did it exhibit any differences related to obstacles in either muscle (Tlat: $t_9 = 1.17$, $P = 0.270$; DP: $t_9 = 1.07$, $P = 0.313$). Similar to rightward perturbations with and without obstacles, we found no learning effects across trials for leftward perturbations with or without the presence of obstacles ($P > 0.05$ by paired t-test, for all muscles). Essentially the same results were observed when subjects ($n = 6$) reached to circular targets with versus without obstacles in the environment (data not shown).

Randomly interleaved trials with and without obstacles. The results described above focused on data collected in a blocked fashion (i.e., blocks of reaching trials to a circular dot separated from trials to a bar). We found essentially the same results as described above when trials with and without obstacles were randomly interleaved ($n = 8$; data not shown). Similar to *experiment 1*, there were no group differences in EMG responses between the randomized and blocked designs ($F_{1,17} = 4.17$, $P = 0.207$, by MANOVA).

Experiment 3: Influence of Tonic Muscle Activity on Feedback Corrections

The purpose of this experiment was to examine the effects of increases in tonic muscle activity upon rapid motor corrections during reaching. Before movement, extensor background loads excited the flexors and caused a significant increase in baseline muscle activity (PM: $t_5 = 2.51$, $P = 0.044$; Br: $t_5 = 3.25$, $P = 0.023$). Similar increases in tonic muscle activity were observed for the extensors before the movement onset for background extensor loads (DP: $t_5 = 5.03$, $P = 0.004$; Tlat: $t_5 = 5.90$, $P = 0.002$). In unperturbed trials, subjects made straight reaching movements with bell-shaped velocity profiles (Fig. 8*A*). Similar hand paths and velocity profiles were observed regardless of the increase in tonic muscle activity (Fig. 8*A*).

Subjects countered perturbations by making corrective movements toward the end goal (Fig. 8*B*). We subtracted the mean of the unperturbed reaching trajectories from that of the mean perturbed trials, effectively removing any increases in tonic muscle activity and isolating the evoked responses (Fig. 8*D*). For Br, there was an increase in the R1 epoch for when a background load was applied, whereas there was no change in activity during the R2 and R3 epochs (R1: $t_5 = -4.07$, $P = 0.009$; R2: $t_5 = -1.95$, $P = 0.108$; R3: $t_5 = -0.65$, $P = 0.549$). For PM, there was no change in the perturbation-related activity with versus without background loads for any of the epochs (R1: $t_5 = 0.835$, $P = 0.442$; R2: $t_5 = 0.69$, $P = 0.524$; R3: $t_5 = -1.45$, $P = 0.986$; Fig. 8*E*).

Essentially the same results were observed for extensor muscles when background loads were applied before the flexor torques. Perturbation-related activity in the R1, R2, and R3 epochs did not change across the different background conditions for DP (R1: $t_5 = 1.37$, $P = 0.230$; R2: $t_5 = -1.18$, $P = 0.292$; R3: $t_5 = -0.53$, $P = 0.622$) and Tlat (R1: $t_5 = -1.36$, $P = 0.232$; R2: $t_5 = -2.36$, $P = 0.065$; R3: $t_5 = -1.30$, $P = 0.249$).

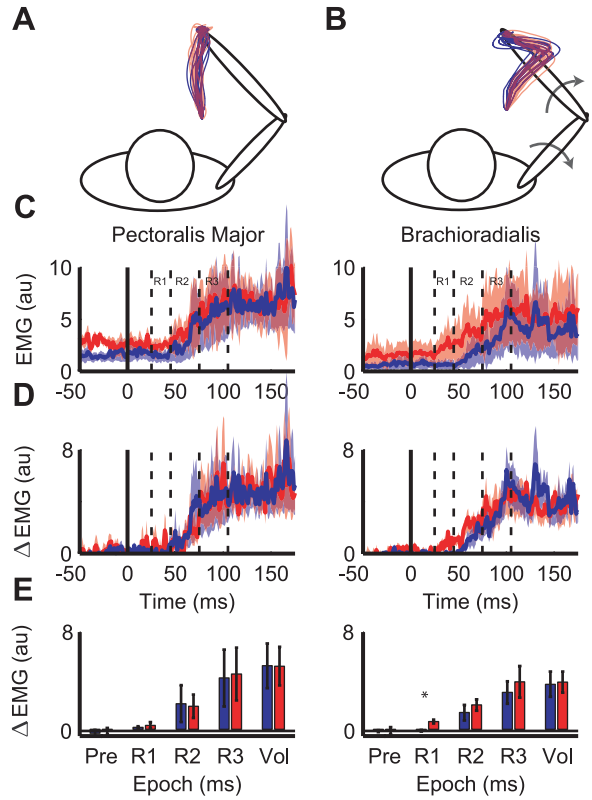

Fig. 8. Kinematics and flexor muscle activity of the bracioradialis (*right*) and pectoralis major (*left*) muscles after extension torque perturbations. *A*: hand motion from an exemplar subject during unperturbed reaching with large (red) and small (blue) background torques. *B*: mean (solid lines) and SE (shaded regions) perturbation hand motions from an exemplar subject during reaching with large (red) and small (blue) background torques. *C*: mean (solid lines) and SE (shaded regions) muscle activity of the bracioradialis (*right*) and pectoralis major (*left*) muscles aligned to the perturbation onset. The blue and red traces indicate the mean muscle activity in the circular dot and rectangular bar, respectively. *D*: mean (solid lines) and SE (shaded regions) perturbation-evoked muscle activity of the group obtained by subtracting each subject's unperturbed muscle activity from their perturbed muscle activity and then averaging across subjects. *E*: bar plots of evoked muscle activity within the different epochs. The vertical height and error bars indicate the group means and SEs, respectively. *$P < 0.05$.

DISCUSSION

Our study highlights how properties of the goal and physical features in the environment modify rapid motor responses after mechanical perturbations applied to the limb. We show that although voluntary motor actions are directed to a central region of a long horizontal goal, corrective responses to a mechanical perturbation were redirected to another spatial location along the goal. Similarly, corrective responses can reroute the hand around obstacles in the environment. Importantly, rightward and leftward perturbations were applied in random order so that the subject had to identify at least the direction of the perturbation to appropriately generate the correct motor response. In both situations, appropriately scaled motor responses occurred in as little as 70 ms.

The use of an optimal control model provides a normative benchmark to quantify how the motor system ought to behave when moving to targets of different shapes and in a cluttered environment. First, the model predicts that the controller should respond to the perturbation as early as possible, even when lateral deviations are not penalized along the bar. This correction occurs even if one dimension of the task space is largely unconstrained because the stabilization at the target requires zero lateral velocity and delaying this response would require more intense control commands. Thus, the best option, given time and cost constraints, is to respond immediately to

changes in external torques with appropriate vigor whether reaching to a bar or to a dot.

Second, motor corrections were goal directed because the controller does not have a desired trajectory. One might say that there is a nominal trajectory that occurs if there were no noise or applied loads. However, the added noise (or load) alters the trajectory, but such deviations do not necessarily lead to corrections back to the nominal trajectory. Rather, corrections only consider the task goals/constraints, reach to the target in a given time period. This leads to goal-directed corrections for perturbed trials and a dispersion in the hand trajectories even for unperturbed trials, as we observed with human motor performance. Admittedly, the ability to compute optimal feedback policies without a desired trajectory is presently only feasible for linear systems. The human limb is clearly nonlinear. However, the lack of mathematical tools at this time does not necessarily mean that humans (or other animals) require desired trajectories to reach to a spatial goal.

Although we applied relatively large perturbations to the limb to generate robust EMG responses, we believe our results reflect online feedback processes used to correct natural motor noise. We have recently shown that EMG responses were measureable and maintained the same timing even for very small perturbations that elicited position and velocity shifts that approached the natural variability observed during unperturbed trials (Crevecoeur et al. 2012). Although not tested here, we believe that the feedback responses based on target shape and the presence/absence of obstacles are also present during unperturbed reaching. This is supported by our observations that end point errors were greater for the bar versus the dot during unperturbed trials.

There was a very small but measureable increase in baseline muscle activity when obstacles were present compared with when they were not present. This suggests that there was slight cocontraction of muscles when obstacles were present. Cocontraction can increase limb stiffness to reduce the effect of perturbations (Franklin and Milner 2003; Franklin et al. 2003, 2007), although the level of cocontraction we observed results in only modest changes in intrinsic muscle stiffness (Pruszynski et al. 2009). An increase in muscle activity is also known to cause an increase in rapid motor responses, typically referred to as "gain scaling," that is largest for the R1 epoch and diminishes in magnitude for later epochs (Verrier 1985; Stein et al. 1995; Pruszynski et al. 2009; Matthews 1986; Marsden et al. 1976; Bedingham and Tatton 1984). Our control experiment highlighted that increases in muscle activity only influenced the R1 response in some muscles and did not affect the long-latency response. Although changes in background loading of one muscle group is not the same as cocontraction of a pair antagonist muscles, it has been demonstrated that perturbation-evoked responses produced in these two conditions are comparable (Carter et al. 1993).

We failed to observe a significant R1 response and consequently found no effect of goal shape or the presence of obstacles on the R1 response. Admittedly, we specifically designed the task (and load magnitudes) to observe motor responses in which the subjects could correct and attain the behavioral goal. Under these conditions, the R1 response was quite small. Beyond gain scaling (described above), there are at least two conditions in which R1 responses appear to be modifiable. First, previous studies have found that extensive practice and direct reinforcement can alter the R1 response (Wolpaw 1983; Wolf and Segal 1996; Christakos et al. 1983). However, feedback of muscle activity was not directly provided in our behavioral task. Second, R1 responses can change for some behaviors such as walking (Komiyama et al. 2000), running (Duysens et al. 1993), and even repetitive arm movements (Capaday and Stein 1986; Zehr et al. 2003). All of these tasks have a common feature in that they are all cyclical in nature, and many studies have highlighted the importance of the spinal cord for locomotor activities (Akazawa et al. 1982; Forssberg et al. 1975). In contrast, we examined motor responses during reaching, a discrete goal-directed task. Previous studies exploring either reaching or maintaining a constant arm posture also did not find changes in R1 responses (Capaday et al. 1994; Colebatch et al. 1976; Crago et al. 1976; Evarts and Granit 1976; Jaeger et al. 1982; Lee and Tatton 1982; Lewis et al. 2006; Rothwell et al. 1980; Hagbarth 1967). This suggests there may be a difference in the properties of short-latency reflexes in cyclical versus noncyclical behaviours (see also Schaal et al. 2004).

We observed context-dependent changes in muscle activity in the R2/R3 response (45–105 ms). Many other studies have highlighted how these long-latency responses have knowledge about the physics of the limb (Kurtzer et al. 2008, 2009; Lacquaniti and Soechting 1984, 1986), compensate for gain scaling (Bedingham and Tatton 1984; Marsden et al. 1976; Matthews 1986; Pruszynski et al. 2009; Stein et al. 1995; Verrier 1985), are altered by verbal instruction (Capaday et al. 1994; Colebatch et al. 1976; Crago et al. 1976; Evarts and Granit 1976; Jaeger et al. 1982; Lee and Tatton 1982; Lewis et al. 2006; Rothwell et al. 1980; Hagbarth 1967), and more recently tuned to the spatial location of a target (Pruszynski et al. 2008). Here, we showed even greater sophistication in these corrective responses including modulation for the characteristics of the goal (size/ shape) and environment (presence of obstacles).

Although spinal and supraspinal pathways contribute to long-latency responses, the task-dependent flexibility observed during this time epoch likely reflects the contribution of a transcortical feedback pathway (Matthews 1991; Scott 2004; Pruszynski et al. 2011a). Neurons in the primary motor cortex respond in as little as 25 ms after perturbations applied to the limb (Herter et al. 2009; Pruszynski et al. 2011a), and the total transmission time to and from the cortex is consistent with the onset of the long-latency epoch (Cheney and Fetz 1984). Primary motor cortex neurons also modulate their activity when the perturbation instructs the monkey to push versus pull on a lever (Evarts and Tanji 1974), an analogous task to the intervene/don't intervene task performed with humans. Transcranial studies on humans have also shown that the primary motor cortex contributes to long-latency motor responses (Day et al. 1991; Pruszynski et al. 2011a).

As the primary motor cortex is also known to be important for voluntary motor control (Porter and Lemon 1993), it is possible that rapid corrective responses generated through the transcortical pathway can take advantage of these voluntary processes. In other words, the known contributions of the primary motor cortex to voluntary control may endow similar qualities to long-latency corrective responses. For example, the distribution of preferred directions of primary motor cortex neurons during reaching are skewed to reflect the physics of limb movement (Scott et al. 2001). Correspondingly, long-latency responses generated

through the transcortical pathway consider the physics of multijoint motion (Pruszynski et al. 2011a).

At the extreme, rapid motor corrections and voluntary control may be effectively the same (Scott 2004). Recent motor control theories suggest that online feedback plays an important role in voluntary motor control (Scott 2004; Todorov and Jordan 2002; Todorov 2004). In this framework, errors in our movements (through noise or environmental forces) are sensed by limb afferents (or more slowly through visual feedback) and combined with efference copy of motor signals to estimate the present state of the limb. This is used to generate motor commands to muscles considering the physical properties of the limb and the behavioral goal. In this framework, the voluntary circuitry is already processing feedback errors all the time. We hypothesize that the discrete mechanical perturbations used in the present study is simply processed through this feedback pathway that is already actively supporting voluntary control of reaching. Sophisticated responses have also been demonstrated for visual feedback corrections during reaching (Franklin and Wolpert 2008; Knill et al. 2011). This intimate relationship between rapid motor responses and voluntary control may explain the difficulty in separating reflexive and voluntary control (Hasan 2005; Prochazka et al. 2000; Rothwell et al. 1980) and why we have chosen to call these corrective actions rapid motor responses rather than reflexes.

Although we focused on the transcortical pathway for interpreting the task-dependent modulation of long-latency responses, there are multiple components to this response (Pruszynski et al. 2011b), so spinal and even other supraspinal pathways likely contribute to muscle activation. Preparatory activity has been observed in the spinal cord before voluntary movement (Prut and Fetz 1999). Presynaptic inhibition has been shown to be generated from descending cortical commands (Carpenter et al. 1963; Andersen et al. 1962, 1964). Therefore, it is possible that the spinal cord could support task-dependent modulations. The question remains as to why short-latency responses that are known to be purely spinal in origin fail to show any task dependency and why the timing of task-dependent modulations in corrective responses parallels transmission times appropriate for the supraspinal pathways (Matthews 1991). Future work is required to help delineate how the various feedback pathways may contribute to support our ability to counter environmental perturbations.

In conclusion, our results highlight that long-latency motor responses are modulated by characteristics of the goal and features of the environment. We hypothesize that such sophistication in feedback responses is generated through feedback pathways that also support voluntary control, notably a transcortical pathway. Therefore, we predict that other aspects of voluntary control will also be present in long-latency responses, such as changes with motor learning and rapid decisional processes that consider the many complex spatial and physical properties of the environment. Correspondingly, the shared nature of voluntary and corrective processing also suggests that the use of discrete mechanical perturbations during voluntary tasks provides a unique probe for studying voluntary control processes.

ACKNOWLEDGMENTS

The authors thank Kim Moore for technical and logistical support.

GRANTS

This work was supported by the National Science and Engineering Research Council of Canada.

DISCLOSURES

S. H. Scott is associated with BKIN Technologies, which commercializes the KINARM robot used in this study.

AUTHOR CONTRIBUTIONS

Author contributions: J.Y.N. and S.H.S. conception and design of research; J.Y.N. and F.C. performed experiments; J.Y.N. analyzed data; J.Y.N. and S.H.S. interpreted results of experiments; J.Y.N. and F.C. prepared figures; J.Y.N. drafted manuscript; J.Y.N., F.C., and S.H.S. edited and revised manuscript; J.Y.N., F.C., and S.H.S. approved final version of manuscript.

REFERENCES

Akazawa K, Aldridge JW, Steeves JD, Stein RB. Modulation of stretch reflexes during locomotion in the mesencephalic cat. *J Physiol* 329: 553–567, 1982.

Akazawa K, Milner TE, Stein RB. Modulation of reflex EMG and stiffness in response to stretch of human finger muscle. *J Neurophysiol* 49: 16–27, 1983.

Andersen P, Eccles JC, Sears TA. Presynaptic inhibitory action of cerebral cortex on the spinal cord. *Nature* 194: 740–741, 1962.

Andersen P, Eccles JC, Sears TA. Cortically evoked depolarization of primary afferent fibers in the spinal cord. *J Neurophysiol* 27: 63–77, 1964.

Bedingham W, Tatton WG. Dependence of EMG responses evoked by imposed wrist displacements on pre-existing activity in the stretched muscles. *Can J Neurol Sci* 11: 272–280, 1984.

Brown IE, Loeb GE. Measured and modeled properties of mammalian skeletal muscle: IV. Dynamics of activation and deactivation. *J Muscle Res Cell Motil* 21: 33–47, 2000.

Capaday C, Forget R, Milner T. A re-examination of the effects of instruction on the long-latency stretch reflex response of the flexor pollicis longus muscle. *Exp Brain Res* 100: 515–521, 1994.

Capaday C, Stein RB. Amplitude modulation of the soleus H-reflex in the human during walking and standing. *J Neurosci* 6: 1308–1313, 1986.

Carpenter D, Lundberg A, Norrsell U. Primary afferent depolarization evoked from the sensorimotor cortex. *Acta Physiol Scand* 59: 126–142, 1963.

Carter RR, Crago PE, Gorman PH. Nonlinear stretch reflex interaction during co-contraction. *J Neurophysiol* 69: 943–952, 1993.

Chapman CS, Goodale MA. Missing in action: the effect of obstacle position and size on avoidance while reaching. *Exp Brain Res* 191: 83–97, 2008.

Cheney PD, Fetz EE. Corticomotoneuronal cells contribute to long-latency stretch reflexes in the rhesus monkey. *J Physiol* 349: 249–272, 1984.

Christakos CN, Wolf H, Meyer-Lohmann J. The "M2" electromyographic response to random perturbations of arm movements is missing in long-trained monkeys. *Neurosci Lett* 41: 295–300, 1983.

Colebatch HJ, Smith MM, Ng CK. Increased elastic recoil as a determinant of pulmonary barotrauma in divers. *Respir Physiol* 26: 55–64, 1976.

Corneil BD, Olivier E, Munoz DP. Visual responses on neck muscles reveal selective gating that prevents express saccades. *Neuron* 42: 831–841, 2004.

Crago PE, Houk JC, Hasan Z. Regulatory actions of human stretch reflex. *J Neurophysiol* 39: 925–935, 1976.

Crevecoeur F, McIntyre J, Thonnard JL, Lefevre P. Movement stability under uncertain internal models of dynamics. *J Neurophysiol* 104: 1401–1408, 2010.

Crevecoeur F, Sepulchre RJ, Thonnard JL, Lefevre P. Improving the state estimation for optimal control of stochastic processes. *Automatica* 47: 591–596, 2011a.

Crevecoeur F, Kurtzer IK, Scott SH. Fast corrective responses are evoked by perturbations approaching the natural variability of posture and movement. *J Neurophysiol* 107: 2821–2832, 2012.

Day BL, Riescher H, Struppler A, Rothwell JC, Marsden CD. Changes in the response to magnetic and electrical stimulation of the motor cortex following muscle stretch in man. *J Physiol* 433: 41–57, 1991.

Diedrichsen J, Dowling N. Bimanual coordination as task-dependent linear control policies. *Hum Mov Sci* 28: 334–347, 2009a.

Diedrichsen J, Gush S. Reversal of bimanual feedback responses with changes in task goal. *J Neurophysiol* 101: 283–288, 2009b.

Duysens J, Tax AA, Trippel M, Dietz V. Increased amplitude of cutaneous reflexes during human running as compared to standing. *Brain Res* 613: 230–238, 1993.
Evarts EV, Granit R. Relations of reflexes and intended movements. *Prog Brain Res* 44: 1–14, 1976.
Evarts EV, Tanji J. Gating of motor cortex reflexes by prior instruction. *Brain Res* 71: 479–494, 1974.
Forssberg H, Grillner S, Rossignol S. Phase dependent reflex reversal during walking in chronic spinal cats. *Brain Res* 85: 103–107, 1975.
Franklin DW, Burdet E, Osu R, Kawato M, Milner TE. Functional significance of stiffness in adaptation of multijoint arm movements to stable and unstable dynamics. *Exp Brain Res* 151: 145–157, 2003.
Franklin DW, Liaw G, Milner TE, Osu R, Burdet E, Kawato M. Endpoint stiffness of the arm is directionally tuned to instability in the environment. *J Neurosci* 27: 7705–7716, 2007.
Franklin DW, Milner TE. Adaptive control of stiffness to stabilize hand position with large loads. *Exp Brain Res* 152: 211–220, 2003.
Franklin DW, Wolpert DM. Specificity of reflex adaptation for task-relevant variability. *J Neurosci* 28: 14165–14175, 2008.
Green DM, Swets JA. *Signal Detection Theory and Psychophysics*. New York: Wiley, 1966.
Hagbarth KE. EMG studies of stretch reflexes in man. *Electroencephalogr Clin Neurophysiol Suppl* 25: 74–79, 1967.
Hammond PH. The influence of prior instruction to the subject on an apparently involuntary neuro-muscular response. *J Physiol* 132: 17P–8P, 1956.
Hasan Z. The human motor control system's response to mechanical perturbation: should it, can it, and does it ensure stability? *J Mot Behav* 37: 484–493, 2005.
Herter TM, Korbel T, Scott SH. Comparison of neural responses in primary motor cortex to transient and continuous loads during posture. *J Neurophysiol* 101: 150–163, 2009.
Howard LA, Tipper SP. Hand deviations away from visual cues: indirect evidence for inhibition. *Exp Brain Res* 113: 144–152, 1997.
Izawa J, Shadmehr R. Online processing of uncertain information in visuomotor control. *J Neurosci* 28: 11360–11368, 2008.
Jackson SR, Jackson GM, Rosicky J. Are non-relevant objects represented in working memory? The effect of non-target objects on reach and grasp kinematics. *Exp Brain Res* 102: 519–530, 1995.
Jaeger RJ, Gottlieb GL, Agarwal GC. Myoelectric responses at flexors and extensors of human wrist to step torque perturbations. *J Neurophysiol* 48: 388–402, 1982.
Knill DC, Bondada A, Chhabra M. Flexible, task-dependent use of sensory feedback to control hand movements. *J Neurosci* 31: 1219–1237, 2011.
Komiyama T, Zehr EP, Stein RB. Absence of nerve specificity in human cutaneous reflexes during standing. *Exp Brain Res* 133: 267–272, 2000.
Krutky MA, Ravichandran VJ, Trumbower RD, Perreault EJ. Interactions between limb and environmental mechanics influence stretch reflex sensitivity in the human arm. *J Neurophysiol* 103: 429–440, 2010.
Kurtzer IL, Pruszynski JA, Scott SH. Long-latency reflexes of the human arm reflect an internal model of limb dynamics. *Curr Biol* 18: 449–453, 2008.
Kurtzer IL, Pruszynski JA, Scott SH. Long-latency responses during reaching account for the mechanical interaction between the shoulder and elbow joints. *J Neurophysiol* 102: 3004–3015, 2009.
Lacquaniti F, Soechting JF. Behavior of the stretch reflex in a multi-jointed limb. *Brain Res* 311: 161–166, 1984.
Lacquaniti F, Soechting JF. Simulation studies on the control of posture and movement in a multi-jointed limb. *Biol Cybern* 54: 367–378, 1986.
Lacquaniti F, Soechting JF, Terzuolo SA. Path constraints on point-to-point arm movements in three-dimensional space. *Neuroscience* 17: 313–324, 1986.
Lametti DR, Houle G, Ostry DJ. Control of movement variability and the regulation of limb impedance. *J Neurophysiol* 98: 3516–3524, 2007.
Lee RG, Tatton WG. Motor responses to sudden limb displacements in primates with specific CNS lesions and in human patients with motor system disorders. *Can J Neurol Sci* 2: 285–293, 1975.
Lee RG, Tatton WG. Long latency reflexes to imposed displacements of the human wrist: dependence on duration of movement. *Exp Brain Res* 45: 207–216, 1982.
Lewis GN, MacKinnon CD, Perreault EJ. The effect of task instruction on the excitability of spinal and supraspinal reflex pathways projecting to the biceps muscle. *Exp Brain Res* 174: 413–425, 2006.
Liu D, Todorov E. Evidence for the flexible sensorimotor strategies predicted by optimal feedback control. *J Neurosci* 27: 9354–9368, 2007.
Marsden CD, Merton PA, Morton HB. Servo action in the human thumb. *J Physiol* 257: 1–44, 1976.
Matthews PB. Observations on the automatic compensation of reflex gain on varying the pre-existing level of motor discharge in man. *J Physiol* 374: 73–90, 1986.
Matthews PB. The human stretch reflex and the motor cortex. *Trends Neurosci* 14: 87–91, 1991.
Mehta B, Schaal SJ. Forward models in visuomotor control. *J Neurophysiol* 88: 942–953, 2002.
Mortimer JA, Webster DD, Dukich TG. Changes in short and long latency stretch responses during the transition from posture to movement. *Brain Res* 229: 337–351, 1981.
Nakazawa K, Yamamoto SI, Yano H. Short- and long-latency reflex responses during different motor tasks in elbow flexor muscles. *Exp Brain Res* 116: 20–28, 1997.
Nichols TR, Houk JC. Improvement in linearity and regulation of stiffness that results from actions of stretch reflex. *J Neurophysiol* 39: 119–142, 1976.
Pierrot-Deseilligny E, Burke D. *The Circuitry of the Spinal Cord: Its Role in Motor Control and Movement Disorders*. Cambridge, UK: Cambridge Univ. Press, 2005.
Porter R, Lemon RN. *Corticospinal Function and Voluntary Movement*. New York: Oxford Univ. Press, 1993.
Prablanc C, Martin O. Automatic control during hand reaching at undetected two dimensional target displacments. *J Neurophysiol* 67: 455–469, 1992.
Prochazka A, Clarac F, Loeb GE, Rothwell JC, Wolpaw JR. What do reflex and voluntary mean? Modern views on an ancient debate. *Exp Brain Res* 130: 417–432, 2000.
Pruszynski JA, Kurtzer I, Lillicrap TP, Scott SH. Temporal evolution of "automatic gain-scaling". *J Neurophysiol* 102: 992–1003, 2009.
Pruszynski JA, King GL, Boisse L, Scott SH, Flanagan JR, Munoz DP. Stimulus-locked responses on human arm muscles reveal a rapid neural pathway linking visual input to arm motor output. *Eur J Neurosci* 32: 1049–1057, 2010.
Pruszynski JA, Kurtzer I, Scott SH. Rapid motor responses are appropriately tuned to the metrics of a visuospatial task. *J Neurophysiol* 100: 224–238, 2008.
Pruszynski JA, Kurtzer IL, Nashed JY, Omrani M, Brouwer B, Scott SH. Primary motor cortex underlies multi-joint integration for fast feedback control. *Nature* 478: 387–390, 2011a.
Pruszynski JA, Kurtzer IL, Scott SH. The long-latency reflex is composed of at least two functionally independent processes. *J Neurophysiol* 106: 449–459, 2011b.
Pruszynski JA, Scott SH. Optimal feedback control and the long-latency stretch response. *Exp Brain Res* 218: 341–359, 2012.
Prut Y, Fetz EE. Primate spinal interneurons show pre-movement instructed delay activity. *Nature* 401: 590–594, 1999.
Rothwell JC, Traub MM, Marsden CD. Influence of voluntary intent on the human long-latency stretch reflex. *Nature* 286: 496–498, 1980.
Scott SH. Apparatus for measuring and perturbing shoulder and elbow joint positions and torques during reaching. *J Neurosci Methods* 89: 119–127, 1999.
Scott SH. Optimal feedback control and the neural basis of volitional motor control. *Nat Rev Neurosci* 5: 532–546, 2004.
Scott SH. Cortical-based neuroprosthetics: when less may be more. *Nat Neurosci* 11: 1245–1246, 2008.
Schaal S, Sternad D, Osu R, Kawato M. Rythmic arm movement is not discrete. *Nat Neurosci* 7: 1136–1143, 2004.
Soechting JF. Effect of target size on spatial and temporal characteristics of a pointing movement in man. *Exp Brain Res* 54: 121–132, 1984.
Stein RB, Hunter IW, Lafontaine SR, Jones LA. Analysis of short-latency reflexes in human elbow flexor muscles. *J Neurophysiol* 73: 1900–1911, 1995.
Todorov E, Jordan MI. Optimal feedback control as a theory of motor coordination. *Nat Neurosci* 5: 1226–1235, 2002.
Todorov E. Optimality principles in sensorimotor control. *Nat Neurosci* 7: 907–915, 2004.
Verrier MC. Alterations in H reflex magnitude by variations in baseline EMG excitability. *Electroencephalogr Clin Neurophysiol* 60: 492–499, 1985.
Wolf SL, Segal RL. Reducing human biceps brachii spinal stretch reflex magnitude. *J Neurophysiol* 75: 1637–1646, 1996.
Wolpaw JR. Adaptive plasticity in the primate spinal stretch reflex: reversal and re-development. *Brain Res* 278: 299–304, 1983.
Zehr EP, Collins DF, Frigon A, Hoogenboom N. Neural control of rhythmic human arm movement: phase dependence and task modulation of hoffmann reflexes in forearm muscles. *J Neurophysiol* 89: 12–21, 2003.